

ON PSEUDOMALACHITE AND CORNETITE

L. G. BERRY*

Queen's University, Kingston, Ontario, Canada

ABSTRACT

New observations combined with existing chemical analyses on pseudomalachite and cornetite from several localities lead to the following description of the two minerals.

Pseudomalachite is monoclinic, prismatic, with space group $P2_1/a$; the unit cell with $a=17.06$, $b=5.76$, $c=4.49\text{A}$, $\beta=91^\circ 02'$, $a:b:c=2.962:1:0.7795$ contains $\text{Cu}_{10}(\text{PO}_4)_4(\text{OH})_8 = 2[\text{Cu}_5(\text{PO}_4)_2(\text{OH})_4]$; calculated specific gravity 4.34. Cleavage (100) perfect and difficult. Specific gravity 4.30–4.35 (coarse crystalline material), 4.08–4.21 (radiating and cryptocrystalline materials). Many specimens labelled pseudomalachite, dihydrite, ehlite, lunnite, tagilite, phosphorochalcite and prasine give the x -ray powder pattern of pseudomalachite.

Cornetite is orthorhombic, dipyramidal, with space group $Pbca$; the unit cell with $a=10.88$, $b=14.10$, $c=7.11\text{A}$, $a:b:c=0.772:1:0.504$. contains $\text{Cu}_{24}(\text{PO}_4)_8(\text{OH})_{24} = 8[\text{Cu}_3\text{PO}_4(\text{OH})_3]$; calculated specific gravity 4.10. Crystals commonly dipyramidal, showing forms $d(210)$, $v(121)$, $n(021)$, $p(221)$ with $(021):(0\bar{2}1)=90^\circ 33'$ (calc.) No cleavage observed. Specific gravity 4.10 (Hutchinson & MacGregor). Ungemach's elements (1929) transformed to the structural setting by $001/200/010$ become $0.7715:1:0.5048$.

PSEUDOMALACHITE— $\text{Cu}_5(\text{PO}_4)_2(\text{OH})_4$

Pseudomalachite, dihydrite, ehlite, lunnite, phosphorochalcite, kupferdiaspore, prasine, and tagilite are among the names found in mineralogical literature for basic copper phosphates, generally similar to malachite in colour.

Wide variation in occurrence as distinct crystals, radiating aggregates and cryptocrystalline crusts together with variation in chemical composition is responsible for the variety of names. Schrauf (1879) proposed the name lunnite for a group including dihydrite, ehlite and phosphorochalcite as members of a series. Dihydrite was retained by Dana (1892) for the distinctly crystalline material and pseudomalachite for the radiating and cryptocrystalline materials.

In the course of this study a large number of museum specimens bearing the above names were examined. The great majority of these specimens yielded an identical x -ray powder pattern, a few proved to be malachite, and two gave patterns which have not been identified. The name pseudomalachite (Hausmann, 1813) which has priority, is retained for this mineral.

Materials and acknowledgements. Most of the specimens were loaned from Harvard Mineralogical Museum (HMM), United States National Museum (USNM), Royal Ontario Museum (ROM), and American Museum of Natural History (AMNH), through the courtesy of Dr. C.

* Associate Professor, Department of Mineralogy.

Frondel, Dr. W. F. Foshag and Mr. E. P. Henderson, Dr. V. B. Meen, and Dr. F. Pough respectively. The following specimens yielded the x-ray powder pattern of pseudomalachite:

1. Pseudomalachite (Queen's University A570) Rheinbreitbach, Germany; dark green sub-spherical radiating aggregates on white and rusty quartz.
2. Dihydrate (ROM, M6762), Ehl, near Linz on the Rhine, Germany; green spherical aggregates in vugs in milky quartz.
3. "Lunnite near pseudomalachite" (HMM, Holden Coll., 100), Rheinbreitbach, Rhenish Prussia; dark green crystals and sub-parallel aggregates with chalcedony in white and rusty fractured quartz.
4. Pseudomalachite (HMM, Holden Coll., 537), Rheinbreitbach, Rhine Province, Germany; dark green aggregates and single crystals (0.5 mm. to 4 mm. long) on iron stained chert.
5. "Dihydrate" (USNM, R5381), Virneberg, Linz, Germany; dark green aggregate of crystals in opening in fractured white and rusty quartz.
6. Pseudomalachite *var.* lunnite (HMM, 61341), Rheinbreitbach; dark green crust 2 mm. thick, coating milky quartz.
7. "Ehlite" (HMM, 90456), Ehl, Germany; rough dark green crystals on yellowish brown cherty matrix.
8. Pseudomalachite (HMM, 61351), Virneberg; radiating aggregates of dark green to black crystals on rusty chert and white milky quartz.
9. "Lunnite" (HMM), Nassau, Germany; dark green radiating aggregate.
10. Pseudomalachite (HMM), Bogoslovsk, Urals; bright green very fine grained radiating aggregate with concentric banding.
11. "Phosphorochalcite" (HMM), Rheinbreitbach; bright green fine grained aggregate with concentric bands, smooth surface with fused appearance.
12. "Lunnite" (USNM, R5388), Rheinbreitbach; dark green radiating groups.
13. "Ehlite" (USNM, R5387) Ehl, Germany; bright green radiating crust.
14. "Tagilite" (HMM, Holden coll., 2970), Nizhni Tagilsk, Ural; bright green and finely crystalline with smooth "fused" surface, with libethenite.
15. "Tagilite" (HMM, 61271), Nischne Tagilsk, Ural; bright green coating.
16. "Ehlite" (HMM, 61391), Ehl near Linz; dark green radiating spherical and sub-spherical aggregates up to 7 mm. diameter on rusty and milky chert.
17. "Prasin" (HMM, Pearce coll.), Libethen, Hungary; dark green botryoidal crust.
18. Pseudomalachite (AMNH, 15329), Rheinbreitbach, Germany; dark green crystalline aggregates on chalcedony.
19. Pseudomalachite (AMNH, 15314), Ehl, Germany; bright green bladed rosettes coated by chalcedony.
20. Pseudomalachite (AMNH, 15325), Cornwall; bright green coating on quartz.
21. "Lunnite" (AMNH, 15322), Virneberg, Germany; dark green crystalline crust on quartz.
22. Pseudomalachite (AMNH, 15323), Libethen, Hungary; dark green compact knobs on quartz and limonite.
23. "Ehlite" (USNM, R5386), Liskeard, Cornwall; bright green coating on quartz.
24. "Dihydrate" (USNM, 103826), Emme Mine, Deserta, Chile; dull green crypto-crystalline material with finely crystalline coating.
25. "Dihydrate" (USNM, C4202), Linz, Prussia; dark green radiating aggregate, $1\frac{1}{4}$ " radius in milky quartz.
26. "Ehlite" (ROM, M15549), Nizhni Tagilsk; bright green radiating aggregate with shiny botryoidal surface and concentric layers, partial outer coating of malachite.

27. "Dihydrate" (AMNH, 15327), Rheinbreitbach; dark green crust coating and coated by quartz.
28. "Tagilite" (HMM, 61281), Tagilsk, Urals; dark green crystalline crust with libethenite and malachite.
29. Pseudomalachite (HMM), Empire-Nevada mine, Yerrington, Nevada; bright green crust.
30. "Dihydrate" (USNM, R5382), Bogollo Portugal; green crust on dark limonitic rock with libethenite.
31. Pseudomalachite, *var. ehliite* (HMM, 61321), Ehl near Linz; bright green crystalline crust on dense milky quartz.
32. "Dihydrate" (USNM, C4201), Rhenish, Prussia; green radiating crust with botryoidal surface and concentric banding.
33. Pseudomalachite, *var. prasine* (HMM, 61371), Libethen, Hungary, green botryoidal crust.
34. "Cornwallite with olivenite" (ROM, M11677), Wheal Unity, St. Day, Cornwall; dark green shiny cryptocrystalline crust with libethenite.
35. "Cornwallite" (HMM, 96231) Wheal Unity, Cornwall, England; green cryptocrystalline crust with libethenite.
36. On cornetite (USNM, R5345), Étoile du Congo, Katanga, bright green spherical aggregates on cornetite.

Physical Properties. Specific gravity determinations, made with the Berman balance, yielded the values given in Table 1. The specific gravity obtained for single crystals or coarse crystalline aggregates (materials 1, 3 and 8) agree closely with values given by Schrauf. The values obtained for finely crystalline radiating aggregates are distinctly lower, suggesting the presence of impurities.

The values for specific gravity given in the literature for analyzed materials are arranged in Table 1 in order of increasing water content. They show a similar variation, many of the higher values are for coarsely crystalline materials while most of the low values are for fine radiating aggregates and cryptocrystalline materials. The specific gravities corresponding to analyses 6, 7, 8 and 13 are not corrected for the malachite shown in the analyses. The colour is lighter for the finer grained materials which usually show a higher water content.

Structural Crystallography. The specimen of pseudomalachite (material 1) at first available to the writer did not show single crystals but yielded a cleavage fragment suitable for single crystal study. This fragment was difficult to orient and did not yield films from which β could be determined. Weissenberg resolutions about a and c indicated a sensibly rectangular lattice but with distinct monoclinic symmetry. Rotation and Weissenberg films about b on materials 2 and 3 readily yielded all the lattice dimensions. Since most crystals on our specimens are quite rough and the β angle is close to 90° , precession camera films about b are particularly valuable for identification of the forms, particularly in distinguishing between (hkl) and $(\bar{h}kl)$. Typical precession films

of the zero layer ($h0l$) and the first layer ($h1l$) are shown in Figs. 1 and 2. The lattice dimensions determined from these films are given in Table 2. The rotation and Weissenberg films were taken with CuK and FeK radiation; CuK and MoK radiations were used for the precession films. The

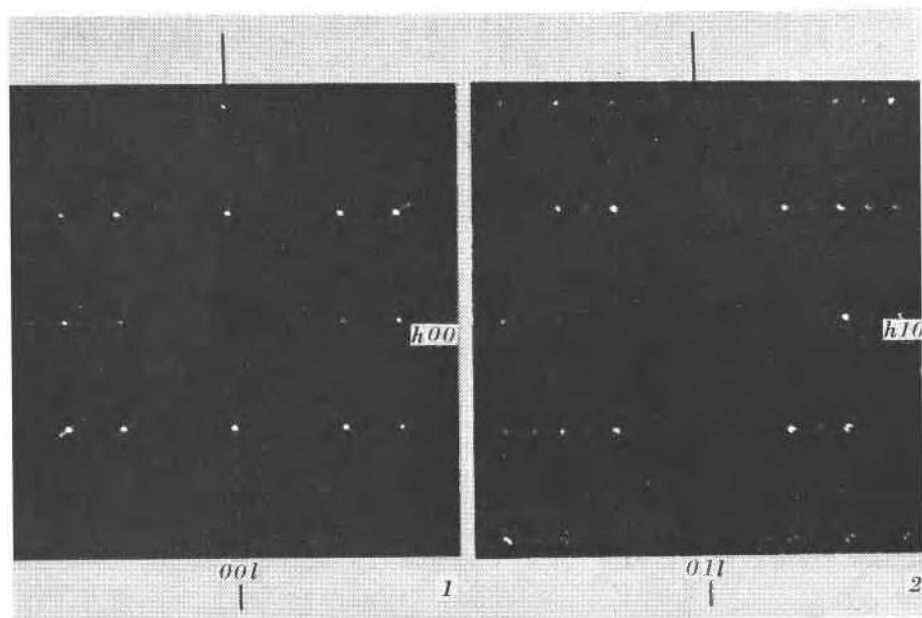
TABLE 1.—PSEUDOMALACHITE: SPECIFIC GRAVITY

New Measurements	
Pseudomalachite, Rheinbreitbach, Germany (material 1)	4.33
"Dihydrate," Ehl, Germany (material 2)	4.15
"Lunnite," Rheinbreitbach (material 3)	4.35
Pseudomalachite, Virneberg (material 8)	4.30
"Lunnite," Nassau, Germany (material 9)	4.21
Pseudomalachite, Bogoslovsk, Urals (material 10)	4.17
"Phosphorochalcite," Rheinbreitbach (material 11)	4.18
"Ehlite," Nizhni Tagilsk, Urals (material 26)	4.08
Old Measurements from Literature	
"Dihydrate," Nizhni Tagilsk (anal. 4)	4.4
"Dihydrate," Rheinbreitbach (anal. 5)	4.309
Pseudomalachite, Nizhni Tagilsk (anal. 6 and 7)	4.24
Pseudomalachite, Nizhni Tagilsk (anal. 8)	4.06
"Phosphorochalcite" Nizhni Tagilsk (anal. 10)	4.25
Pseudomalachite, Katanga (anal. 11)	3.58
Pseudomalachite, Nizhni Tagilsk (anal. 13)	4.13
"Ehlite," Ehl (anal. 3 and 15)	4.1024
Pseudomalachite, Nizhni Tagilsk (anal. 17)	4.175
"Phosphorochalcite," Virneberg (anal. 18)	4.40
Pseudomalachite, Libethen (anal. 19)	4.1556
"Prasine" (anal. 22)	3.98
"Lunnite," Cornwall (anal. 23)	4.25
"Ehlite," Cornwall (anal. 24, 33, 35)	3.911 to 4.23
"Phosphorochalcite," Virneberg (anal. 26)	4.2 to 4.4
"Phosphorochalcite," Nizhni Tagilsk (anal. 27)	4.0
"Ehlite," Ehl (anal. 31 or 32)	4.198
"Ehlite," Nizhni Tagilsk (anal. 38)	3.80
"Tagilite," Nizhni Tagilsk (anal. 39)	3.50

β angle was deduced from the measured spacings of (100), (001), (401), ($\bar{4}01$), (601), and ($\bar{6}01$), as well as from direct measurement on Weissenberg and precession resolutions of the zero layer ($h0l$).

The values obtained for the lattice dimensions agree well with the average values:

$$a=17.06, b=5.76, c=4.49 \text{ \AA}, \beta=91^{\circ}02$$



FIGS. 1, 2. Pseudomalachite, Rheinbreitbach, Germany (material 3): x -ray precession photographs with $\text{CuK}\alpha$ radiation; film to specimen distance 60 mm. reproduced $\frac{2}{3}$ actual size. FIG. 1. The zero level ($h0l$) showing diffractions present only with $h=2n$ characteristic of the space group $P2_1/a$. FIG. 2. The first level ($h1l$) with all diffractions present. Both films show the near orthorhombic character of the lattice with $\mu=88^\circ58'$.

TABLE 2. PSEUDOMALACHITE: LATTICE DIMENSIONS¹

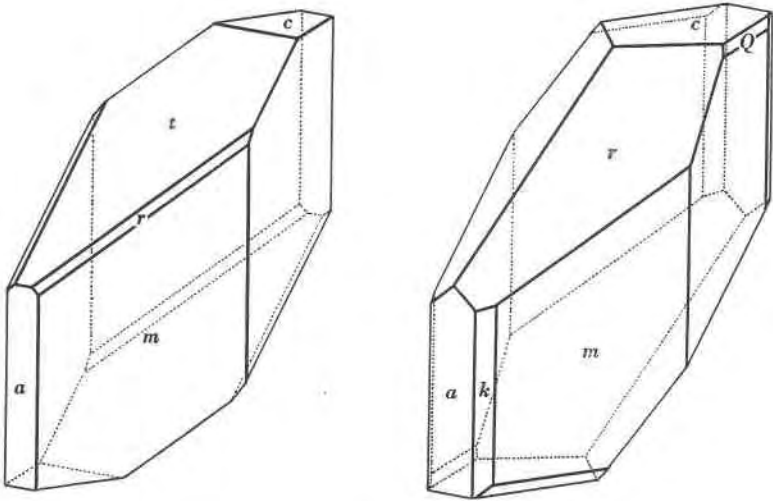
Material	Type of Films	a	b	c	β
1	Rotation, Weissenberg about a and b	17.03 A	5.76 A	4.49 A	$90^\circ \pm 1^\circ$
2	Rotation, Weissenberg about b and c	17.10	5.76	4.49	$90^\circ 57'$
3	Rotation, Weissenberg about b	17.04	5.75	4.48	91 01
	Precession about b	17.08	—	4.49	91 00
4	Precession about b	17.02	—	4.50	[91 32]
5	Precession about b & c	17.08	5.75	4.47	91 07
8	Precession about b & c	[17.16]	5.77	4.49	[91 22]
31	Precession about b & c	[17.14]	5.76	4.49	91 05
Average*		17.06	5.76	4.49	$90^\circ 02'$

¹ Using $\text{CuK}\alpha$ 1.5418, $\text{FeK}\alpha$ 1.9373, $\text{MoK}\alpha$ 0.7107 A, mass factor 1.6602.

* Omitting bracketed values.

The observed diffractions conform to the conditions: (hkl) present in all orders, $(h0l)$ present only with $h=2n$, $(0k0)$ present with $k=2n$; these criteria are characteristic for the space group. $C_{2h}^5 - P2_1/a$.

Geometrical Crystallography. Single crystals occur on several of the available specimens of pseudomalachite and a number of these were mounted for measurement on the two-circle goniometer. On most crystals only the faces of the pinacoid $a(100)$ give good reflections, other faces are usually rough, rounded, or rarely striated. Most of these crystals



FIGS. 3, 4. Pseudomalachite, crystal drawings. FIG. 3 (left). Rheinbreitnbach, Germany (material 4), showing the forms $c(001)$, $a(100)$, $m(110)$, $t(201)$ and $r(311)$. FIG. 4 (right). Virneberg, Linz, Germany (materials 5 and 8), showing the forms $c(001)$, $a(100)$, $m(110)$, $k(210)$, $r(311)$ and $Q(\bar{3}31)$ or $(\bar{1}0.8.3)$.

were adjusted on the goniometer with (100) polar and measured in that position. The measured angles for materials 4, 5, 27 and 31, clearly very poor, were converted to ϕ , ρ angles graphically on a stereographic net. The indexing of the terminal faces was clearly established by a zero layer precession photograph about the b -axis of one of the measured crystals of materials 4, 5 and 31. The crystals from material 3, although usually fragments from subparallel aggregates, are quite sharp and most faces give fair signals, $a(100)$ and $T(\bar{2}01)$ give excellent signals. Fully developed crystals are not present on material 3, all the measured crystals show only $(\bar{h}0l)$ and $(\bar{h}kl)$ terminal faces and no crystals show the faces (001) and (100) intersecting. Fig. 3 illustrates a typical crystal of material 4 and Fig. 4 a typical crystal of materials 5 and 8. In Table 3, the measured ϕ_2 and ρ_2 angles for material 3 are given together with

ϕ and ρ angles obtained stereographically from angles measured with (100) polar for crystals of other materials. With the latter crystals, the original measurements are so poor that no loss of accuracy results from this procedure. The ($hk0$) faces, which are very rough and rounded, have been indexed as $m(110)$ although the measured ϕ angles differ by 4° to 6° from the calculated angles. The indexing of these forms is therefore quite rough.

The measured angles for material 3 give rather widely divergent values for the polar elements; which in turn yield the average values:

$$r_2:p_2:q_2=1.239:0.3422:1; \mu=87^\circ 58'$$

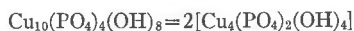
The axial ratio, obtained from these polar elements, agrees poorly with the triclinic elements given by Schrauf (1879) and the structural lattice axial ratio:

$$\begin{aligned} a:b:c &= 2.924 : 1:0.808 & \beta &= 92^\circ 02' \text{ (goniometric)} \\ a:b:c/2 &= 2.8252:1:0.7669 & \alpha &= 89^\circ 29\frac{1}{2}' & \beta &= 91^\circ 00\frac{1}{2}' & \gamma &= 90^\circ 39\frac{1}{2}' \text{ (Schrauf)} \\ a:b:c &= 2.962 : 1:0.7795 & \beta &= 91^\circ 02' \text{ (x-ray)} \end{aligned}$$

The majority of published drawings of pseudomalachite crystals together with the crystals studied here clearly suggest monoclinic symmetry; this is now confirmed by the x -ray films. The measured interfacial angles given by Schrauf when considered in the light of known monoclinic symmetry, show inconsistencies similar to those in the measured angles given here. Schrauf took the inconsistencies seriously and deduced triclinic elements with interaxial angles close to 90° ; he also gave rather improbably indices to some faces. It is, therefore, proposed that the structural lattice axial ratio best represents crystals of pseudomalachite. These elements have been used to calculate the following angle table (Table 4).

A comparison of the measured angles with the calculated angles reveals fair agreement for a few forms but generally poor for most forms. Schrauf's symbols are converted to the structural setting by dividing the l index by 2.

Composition and cell content. The structural lattice dimensions combined with the measured specific gravity (4.309) and chemical analysis of the crystalline material ("dihydrate") from Rheinbreitbach, Germany (Schrauf, 1879) gives the numbers of atoms in the unit cell (Table 5). The number of atoms (3) clearly indicate the structural formula:



with the ideal numbers of atoms in column 4. The specific gravity calculated for this structural formula is 4.34 in close agreement with the measured values for well crystallized specimens (Table 1).

TABLE 3. PSEUDOMALACHITE: CRYSTAL MEASUREMENTS

Rheinbreitinbach (material 3)—8 crystals						
Form	Number of Faces	Quality	Average		Range	
			ϕ_2	ρ_2	ϕ_2	ρ_2
<i>c</i> (001)	5	good	89° 27'	90° 00'	89° 04'–89° 43'	—
<i>a</i> (100)	5	good	0 00	90 00	—	—
<i>m</i> (110)	5	rough	0 00	19 23	—	18° 55'–20° 49'
<i>k</i> (210)	4	striated	0 00	33 47	—	33 14–34 11
<i>j</i> (310)	1	striated	0 00	40 00	—	—
<i>T</i> (201)	7	good	116 50	90 00	116 43–116 59	—
<i>D</i> ($\bar{4}$ 43)	3	rough	108 40	48 05	108 06–108 48	46 40–49 20
<i>S</i> ($\bar{3}$ 12)	1	rough	110 57	72 05	—	—
<i>R</i> ($\bar{3}$ 11)	6	rough	127 39	57 18	126 21–129 44	56 18–58 08
($\bar{1}$ 2.3.2)	3	rough	146 04	55 44	145 44–146 29	54 39–56 19

Rheinbreitinbach (material 4)—2 crystals				
Form	Number of Faces	Quality	ϕ	ρ
<i>c</i> (001)	2	very rough	90°	1° 26'
<i>a</i> (100)	2	good	90	90
<i>m</i> (110)	4	rough, rounded	24½	90
<i>t</i> (201)	2	rough	90	29
<i>r</i> (311)	4	rough	46	48½

Virneberg, Linz, Germany (material 5)—2 crystals				
Form	Number of Faces	Quality	ϕ	ρ
<i>c</i> (001)	2	very rough	90	3°
<i>b</i> (010)	1	narrow	0	90
<i>a</i> (100)	2	good	90	90
<i>m</i> (110)	6	large, rough	22	90
<i>k</i> (210)	4	narrow	36	90
<i>r</i> (311)	3	large, rough	42	53
($\bar{1}$ 0.8.3)	4	narrow line	–23	65

Rheinbreitinbach (material 27)—1 crystal				
Form	Number of Faces	Quality	ϕ	ρ
<i>a</i> (100)	1	good	90	90
<i>m</i> (110)	2	rough, rounded	18½	90
<i>t</i> (201)	1	large, rough	90	31½
<i>u</i> (601)	1	small, rough	90	59½
<i>r</i> (311)	1	rough	46½	48½

TABLE 3—continued

Ehl, Linz, Germany (material 31)—3 crystals				
<i>c</i> (001)	2	very rough	90	1½
<i>a</i> (100)	4	fair	90	90
<i>m</i> (110)	9	rough	21½	90
<i>e</i> (021)	4	narrow	6	53
<i>r</i> (311)	6	rough	47½	4
<i>D</i> (443)	3	rough	-21	48

TABLE 4. PSEUDOMALACHITE: $\text{Cu}_5(\text{PO}_4)_2(\text{OH})_4$ Monoclinic, $P2_1/a$ $a:b:c = 2.962:1:0.7795$; $\beta = 91^\circ 02'$, $r_2:p_2:q_2 = 1.283:0.3376:1$ $p_0:q_0:r_0 = 0.2632:0.7795:1$; $\mu = 88^\circ 58'$, $p_0' = 0.2632$, $q_0' = 0.7795$, $x_0' = 0.0180$

Form	ϕ	ρ	ϕ_2	$\rho_2 = B$	C	A
<i>c</i> (001)	90° 00'	1° 02'	88° 58'	90° 00'	0° 00'	88° 58'
<i>b</i> (010)	0 00	90 00	—	0 00	90 00	90 00
<i>a</i> (100)	90 00	90 00	0 00	90 00	88 58	0 00
<i>m</i> (110)	18 39½	90 00	0 00	18 39½	89 40	71 20½
<i>n</i> (540)	22 53	90 00	0 00	22 53	89 36	67 07
<i>l</i> (430)	24 14½	90 00	0 00	24 14½	89 34½	65 45½
<i>k</i> (210)	34 02	90 00	0 00	34 02	89 25½	55 58
<i>j</i> (310)	45 22	90 00	0 00	45 22	89 16	44 38
<i>e</i> (021)	0 40	57 19½	88 58	32 41	57 19	89 26½
<i>t</i> (201)	90 00	28 34	61 26	90 00	27 32	61 26
<i>u</i> (601)	90 00	57 57	32 03	90 00	56 55	32 03
<i>T</i> (201)	-90 00	26 57	116 57	90 00	27 59	116 57
<i>f</i> (332)	19 27	51 07	67 34	42 46½	50 46½	74 59
<i>P</i> (111)	-17 27½	39 15½	103 46½	52 52	39 34½	100 57
<i>D</i> (443)	-17 45½	47 30	108 25	45 24	47 49½	103 00
<i>Q</i> (331)	-18 15½	67 54	127 39	28 22½	68 13½	106 52½
<i>h</i> (432)	24 58	52 12½	61 26	44 14½	51 47	70 31
<i>r</i> (311)	46 01	48 18	51 04½	58 46	47 34	57 30½
<i>S</i> (312)	-44 02	28 27½	110 39	69 58	29 11	109 21½
<i>H</i> (432)	-23 30	51 53½	116 57	43 49	52 18½	108 17
<i>R</i> (311)	-44 42½	47 38½	127 39	58 19	48 22½	121 19½
(10.8.3)	-22 53	66 06	131 16½	32 37	66 30½	110 49½
(12.3.2)	-53 10	62 51½	147 21½	57 46	63 41	135 25

TABLE 6—continued

	33	34	35	36	37	38	39	A	B
Cu	9.21	9.09	9.21	10.22	8.06	9.12	8.09	9.61	10
P	3.70	2.84	3.67	3.21	4.01	3.54	3.91	3.72	4
V	—	0.90	—	—	—	—	—		
H	11.12	11.12	11.24	11.32	11.82	12.05	12.26	10.16	8
O	24.00	24.00	24.00	24.00	24.00	24.00	24.00	24.00	24

1. "Dihydrate," Rheinbreitenbach, Germany; anal. Arvedson (1825), in Dana (1892, p. 794, no. 2). 2. Pseudomalachite ("Kupferdiaspore"), Libethen, Hungary, fibrous, radiating; anal. Kühn (1844) (Dana, no. 22). 3. "Dihydrate," Eh., Germany; anal. Schrauf (1879, p. 14) from analysis 10 after deducting chrysocolla (Schrauf, 1879). 4. "Dihydrate," Nizhni Tagilsk, Russia, crystals; anal. Hermann (1846), (Dana, no. 1). 5. "Dihydrate," Rheinbreitenbach, hemispherical aggregates, crystals; anal. Schrauf (1879) (Dana, no. 3). 6, 7, 8 and 9. Nischni Tagilsk; anal. Nordenskiöld (1858), less malachite on basis of CO_2 given in analysis; 6 & 7. not distinctly crystallized; 8. compact massive; 9. nearly amorphous; in part in Dana (1882). 10. "Phosphorochalcite," Nizhni Tagilsk, nodules and tubular masses with fibrous structure; anal. Hermann (1846) (Dana, no. 9). 11. Pseudomalachite, Katanga, Belgian Congo, banded, fibrous masses; anal. Cesàro & Bellière (1922). 12. Pseudomalachite, Herschberg, spherical and radiating groups, anal. Kühn (1840) (Dana, no. 16). 13. Nizhni Tagilsk, fine fibrous; anal. Nordenskiöld (1858) in Dana (1882), after deducting 4.07% malachite. 14. Pseudomalachite, Rheinbreitenbach, fibrous; anal. Bergemann (1828). 15. "Ehlite," Eh.; anal. Schrauf (1879) (Dana, no. 15). 16. Phosphorochalcite, Linz; anal. Bergemann (1858) (Dana, no. 19). 17. Pseudomalachite, Nizhni Tagilsk, concentric layer structure; anal. Schrauf (1879) (Dana no. 20). 18. "Phosphorochalcite," Virneberg, spherical radiating masses; anal. Hermann (1846) (Dana, no. 4). 19. Pseudomalachite, Libethen, radiating concentric aggregates; anal. Schrauf (1879) (Dana, no. 21). 20. "Ehlite," Rheinbreitenbach, dark green spherical masses; anal. Bergemann (1828). 21. Pseudomalachite, Las Coste, fibrous reniform concretions; anal. La Croix (1910). 22. "Prasine," radiating botryoidal shells; anal. Maskelyne & Flight (1872) (Dana, no. 11). 23. "Lunnite," Cornwall; minute radiating spheres; anal. Heddle (1855) (Dana, no. 8). 24. "Ehlite," Cornwall, radiating globules; anal. Church (1873) (Dana, no. 12). 25. "Ehlite," Rheinbreitenbach, spherical masses; anal. Bergemann (1828). 26. "Phosphorochalcite," Virneberg, near Rheinbreitenbach; anal. Rhodius (1847). 27. "Phosphorochalcite," Nizhni Tagilsk, lamellar masses with curved radiating structure; anal. Hermann (1846). 28. "Ehlite," Nizhni Tagilsk; anal. Wendel in Rammelsberg (1875) (Dana no. 10). 29. "Ehlite," Eh.; anal. Bergemann (1828) (Dana, no. 6). 30. "Phosphorochalcite," Rheinbreitenbach, dense masses; average of 3 analyses, Kühn (1844) (Dana, no. 17). 31. "Ehlite," Eh.; anal. Nordenskiöld (1858) (Dana, 1882, no. 4). 32. "Ehlite," Eh.; anal. Nordenskiöld in Rammelsberg (1860) (Dana, no. 5). 33. "Ehlite," Cornwall; anal. Church (1873) (Dana no. 14). 34. "Ehlite," Eh.; anal. Bergemann (1858) (Dana, no. 7). 35. "Ehlite," Cornwall; anal. Church (1873) (Dana, no. 13). 36. "Prasine," Libethen; anal. Church (1864) (Dana, no. 18). 37. "Tagilite," Mercedes mine, Coquimbo, Chile, stellated and fibrous masses on limonite; anal. Field (1859) in Dana (1892). 38. "Ehlite," Nizhni Tagilsk; anal. Hermann (1846). 39. "Tagilite," Nizhni Tagilsk; anal. Hermann (1846) in Dana (1892), less 1.75% limonite. A. Average cell content from 39 analyses. B. Ideal cell content for $2[\text{Cu}_5(\text{PO}_4)_2(\text{OH})_4]$.

The numerous published analyses of pseudomalachite show considerable variation and have led to several empirical formulae. The empirical formula $\text{Cu}_5\text{P}_2\text{H}_4\text{O}_{12}$ proposed by Schrauf for dihydrite is confirmed by the unit cell content. Other formulae have been deduced from analyses showing higher water content.

The available analyses of pseudomalachite in Table 6 which have been reduced to atomic proportions on the basis of 24 oxygen atoms are arranged in order of increasing H content. The average numbers of atoms (column A) agree reasonably well with the ideal cell content except in the number for H which is close to 10. In many cases the apparent high water content is probably due to admixed malachite which is a very common associate especially at Nizhni Tagilsk, Siberia. Nordenskiöld's analyses (6, 7, 8, 9, 13) of this material, which all show CO_2 , fit the ideal cell content fairly well when malachite is deducted. Chrysocolla, deducted by Schrauf from analysis 10 resulting in analysis 3, may be present in other analysed materials. The cryptocrystalline materials appeared homogeneous and identical with the crystalline upon examination by x -ray powder patterns.

Optical Properties. Optical data for pseudomalachite have been published by Larsen (1921) and by Barth & Berman (1930). The Harvard Museum specimens for which Barth & Berman (1930) give optical data were fortunately available for x -ray study. Three of these specimens (materials 6, 7, 8 in Table 7) with closely similar optical properties gave the characteristic powder pattern of pseudomalachite. The fourth (HMM 90455) gave the pattern of malachite; the optical data also agree closely with those for malachite. The optical data given by Larsen (1921) differ rather markedly from the others. Unfortunately Larsen's specimens were not available for x -ray study. Crystals of materials 3 and 5 which had been oriented on the precession camera were mounted on the universal stage for measurement of the extinction angle. The X direction lies in the obtuse angle β in both cases.

X-ray Powder Pattern. All the materials listed in the first part of this paper yield an identical x -ray powder pattern (Figs. 5, 6). The films of materials 2, 3 and 9 were carefully measured. Materials 2 and 3 were coarsely crystalline and yielded material for single crystal study while material 9 is a fibrous radiating aggregate. The estimated intensities, measured θ and d values given in Table 8 were averaged from closely similar measurements on the three films. The films for materials 2 and 9 showed many back reflection rings providing a check on film shrinkage. The recorded diffractions for θ greater than 37° occurred only on these two films. A few weak diffractions which were only observed on one of the two films were omitted from the table. The pattern has been indexed

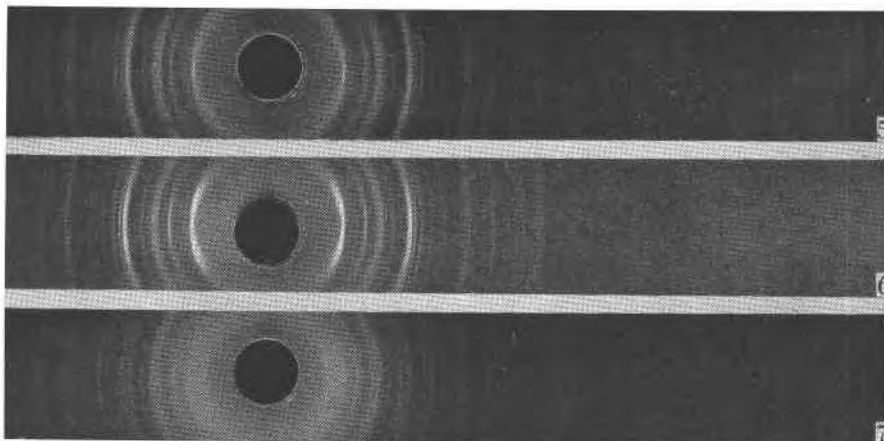
TABLE 7. PSEUDOMALACHITE: OPTICAL DATA, $Z=b$

α	β	γ	2V	$c \wedge X$	Material and Observer
—	—	—	—	21°	material 3, L.G.B.
—	—	—	—	26°	material 5, L.G.B.
1.789	1.835	1.845	50°±	21°	material 6, Barth & Berman (1930)
1.785	1.850	1.862	50°±	21°	material 7, Barth & Berman (1930)
1.80	1.86	1.88	46°	23°	material 8, Barth & Berman (1930)
1.719	1.763	1.805	90°±	—	Bogolo, Portugal, Larsen (1921)
1.73	—	1.807	—	—	Hungary, Larsen (1921)

TABLE 8. PSEUDOMALACHITE— $\text{Cu}_5(\text{PO}_4)_2(\text{OH})_4$: X-RAY POWDER PATTERN
Monoclinic, $P2_1/a$; $a=17.06$, $b=5.76$, $c=4.49$ A, $\beta=91^\circ 02'$; $Z=2$

I	$\theta(\text{Cu})$	$d(\text{meas.})$	(hkl)	$d(\text{calc.})$	I	$\theta(\text{Cu})$	$d(\text{meas.})$	(hkl)	$d(\text{calc.})$			
$\frac{1}{2}$	9.33°	4.75 A	(210)	4.770 A	1	17.55°	2.56 A	(320)	2.569 A			
10	9.92	4.48	(001)	4.489				(610)	2.543			
5	12.87	3.46	($\bar{1}$ 11)	3.477				(021)	2.424			
			(410)	3.425				($\bar{6}$ 01)	2.421			
$\frac{1}{2}$	13.64	3.27	(211)	3.254				8	18.85	2.39	(121)	2.397
2	14.29	3.12	($\bar{4}$ 01)	3.120							(420)	2.388
4	14.43	3.09	(401)	3.064				5	19.38	2.32	(601)	2.382
2	14.69	3.04	($\bar{3}$ 11)	3.025							(221)	2.337
4	15.03	2.97	(311)	2.987				5	20.19	2.23	(221)	2.325
3	15.24	2.93	(510)	2.933							(002)	2.245
1	15.71	2.85	(600)	2.843	5	20.19	2.23	(710)	2.243			
			(120)	2.838				(321)	2.237			
3	16.43	2.72	(220)	2.729				($\bar{6}$ 11)	2.232			
			(411)	2.705				(321)	2.221			

I	$\theta(\text{Cu})$	$d(\text{meas.})$	I	$\theta(\text{Cu})$	$d(\text{meas.})$	I	$\theta(\text{Cu})$	$d(\text{meas.})$
1	20.61°	2.19 A	2	31.14°	1.491 A	1	51.51°	0.985 A
1	21.31	2.12	1	31.81	1.462	1	53.52	0.958
3	21.66	2.09	3	32.57	1.431	1	55.42	0.936
1	22.56	2.01	3	32.91	1.419	2	58.63	0.903
2	23.13	1.963	4	33.64	1.392	1	61.09	0.880
1	23.42	1.939	1	34.37	1.365	2	62.25	0.871
2	24.56	1.854	2	34.81	1.350	1	64.27	0.856
4	25.93	1.763	3	35.28	1.335	1	67.61	0.834
5	26.5	1.728	2	35.75	1.319	1	69.26	0.824
2	27.47	1.670	3	36.02	1.310	1	71.52	0.813
1	28.33	1.624	1	39.48	1.212	1	72.18	0.810
2	28.87	1.597	1	40.13	1.196	2	72.77	0.807
4	29.64	1.559	$\frac{1}{2}$	45.75	1.076	1	73.28	0.804
2	30.32	1.527	3	47.91	1.039	1	73.87	0.802
2	30.96	1.498	3	49.46	1.014	3	76.34	0.794



FIGS. 5, 6, 7. X-ray powder photographs with Cu/Ni radiation; camera radius $90/\pi$ mm. ($1^\circ\theta=1$ mm. on film); full size reproduction of contact prints. FIG. 5. Pseudomalachite, Rheinbreitbach, Germany; coarse crystalline (material 1). FIG. 6. Pseudomalachite, Nassau, Germany; radiating fibrous aggregate (material 9). FIG. 7. Cornetite, Bwana Mkubwa, Northern Rhodesia.

as far as $\theta=20.19^\circ$ and the measured spacings agree closely with one or more calculated values.

CORNETITE— $\text{Cu}_3\text{PO}_4(\text{OH})_3$

Cornetite was first described by Cesàro (1912*a*, *b*) from the copper mine L'Étoile du Congo, Katanga, Belgian Congo and by Hutchinson & MacGregor (1913, 1921) from Bwana Mkubwa, Northern Rhodesia. Cesàro (1912*b*) described the chemical composition as "essentiellement d'un phosphate de cuivre et de cobalt"; the name cornetite was given by Buttgenbach (1916) to the material described by Cesàro. Hutchinson & MacGregor (1913, 1921) give a chemical analysis of their material yielding the empirical formula $2\text{Cu}_3(\text{PO}_4)_2 \cdot 7\text{Cu}(\text{OH})_2$. In the later communication these authors (1921) recognize their material as cornetite and conclude that the material described by Cesàro differs only in a small content of cobalt. Schoep (1922) re-examined cornetite from L'Étoile du Congo, Katanga and proved conclusively that cobalt is not a constituent of the cornetite crystals.

The observations given in this paper were obtained from crystals on a typical specimen from Bwana Mkubwa, Northern Rhodesia, from the mineralogical collections of Queen's University. The mineral occurs as an incrustation of peacock blue crystals up to $0.3 \times 0.3 \times 0.2$ mm. underlain by a thin layer of brownish black material on compact, grey argil-

laceous sandstone. The specimen is similar in nearly every respect to one specimen described by Hutchinson & MacGregor (1921) from the same locality.

Two additional specimens (USNM R5345 and ROM M13540) from Étoile du Congo, Katanga, Belgian Congo, were also examined. These specimens consisted of small blue crystals and crystal aggregates partially embedded in fine grained argillaceous sandstone. On one specimen a few small spherical aggregates of pseudomalachite are implanted on top of the cornetite crystals.

Structural Crystallography. Crystals of cornetite on our specimen from Bwana Mkubwa are ideally suited for single crystal x -ray studies. Rotation, zero and first layer Weissenberg photographs about $c[001]$ and $a[100]$ and a rotation film about $b[010]$ indicate orthorhombic symmetry in the Laue class $D_{2h}-mmm$ and lead to an orthorhombic cell:

$$a=10.88, b=14.10, c=7.11 \text{ \AA.}$$

The observed diffractions conform to the conditions: (hkl) present in all orders; $(0kl)$ present only with $k=2n$; $(h0l)$ present only with $l=2n$; $(hk0)$ present only with $h=2n$. These conditions are characteristic of the space group $D_{2h}^{1p}-Pbca$.

Rotation and zero-layer Weissenberg films about $[0\bar{1}2]$ on one crystal of cornetite from Katanga give $a=10.85 \text{ \AA}$ and other values in close agreement with values calculated from the above structural elements.

Geometrical Crystallography. Cesàro (1912*b*), Hutchinson & MacGregor (1913, 1921), Schoep (1927) and Ungemach (1929) give crystal measurements for cornetite and deduce orthorhombic elements in three different settings. Hutchinson & MacGregor (1921) and Schoep (1927) retain Cesàro's setting and elements. Ungemach lists the same forms recorded by Cesàro together with 6 new forms. From excellent measured angles $(110)\wedge(1\bar{1}0)$ and $(021)\wedge(0\bar{2}1)$ he obtains the axial ratio:

$$a:b:c=0.99045:1:1.5282$$

in Cesàro's setting but with the c -axis doubled to give more normal symbols. The morphological lattices are related to the structural lattice by the reversible transformation formulae:

Cesàro (1912 <i>b</i>), Hutchinson & MacGregor (1921) to Berry	001/100/0 $\frac{1}{2}$ 0
Berry to Cesàro (1912 <i>b</i>), Hutchinson & MacGregor (1921)	010/002/100
Hutchinson & MacGregor (1913) to Berry	100/0 $\frac{1}{2}$ 0/00 $\frac{1}{4}$
Berry to Hutchinson & MacGregor (1913)	100/020/004
Ungemach to Berry	001/200/010
Berry to Ungemach	0 $\frac{1}{2}$ 0/001/100

The geometrical axial ratios transformed into the structural setting compare closely with the structural lattice axial ratio:

$$\begin{aligned}
 a:b:c &= 0.773 : 1 : 0.504 \quad (\text{structural lattice}) \\
 c:a:b/2 &= 0.7801 : 1 : 0.5079 \quad (\text{Cesàro, 1912b}) \\
 2a:b:c/2 &= 0.788 : 1 : 0.505 \quad (\text{Hutchinson \& MacGregor, 1913}) \\
 c:a:b/2 &= 0.7703 : 1 : 0.5074 \quad (\text{Hutchinson \& MacGregor, 1921}) \\
 c/2:a:b/2 &= 0.7715 : 1 : 0.5048 \quad (\text{Ungemach, 1929})
 \end{aligned}$$

The close agreement between the structural lattice elements and the elements deduced by Ungemach from careful measurements on a number of crystals indicates that the latter elements best represent crystals of cornetite. Table 9 gives the observed forms of cornetite with their indices in the structural setting. In Table 10 the two circle angles, calculated from Ungemach's elements in the structural setting, are given for all the forms observed on cornetite crystals.

TABLE 9. CORNETITE: OBSERVED FORMS

Cesàro (1912b)	Hutchinson & MacGregor (1913)	(1921)	Ungemach (1929)	Berry
—	—	—	g' (010)	c (001)
a (100)†	—	—	—	b (010)
—	—	—	p (001)	a (100)
—	—	—	a^2 (102)	m (110)
a^2 (102)	(110)	d (102)	a^1 (104)	d (210)
m (110)	(011)	m (110)	m (110)	n (021)
—	—	—	$e^{1/2}$ (021)	e (102)
$b^{1/4}$ (221)	—	v (221)	$b^{1/2}$ (111)	v (121)
$b^{1/2}$ (111)	—	p (111)	b^1 (112)	p (221)
—	—	—	$b^{3/2}$ (113)	r (321)
—	—	—	b^2 (114)	s (421)
—	—	—	—	t (521)*

* New form observed on one crystal from Katanga.

† Observed by Schoep (1927).

The crystals of cornetite from Northern Rhodesia, used in this study, show the forms d (210), n (021), v (121) and p (221). A typical crystal is illustrated in Fig. 8. Measured angles on these crystals agree closely with Ungemach's calculated angles. One crystal fragment of cornetite from Katanga (ROM M13540) which was mounted for x -ray measurements shows the forms n (021), v (121), p (221) and one face with indices (521). The measured angles for this face, compared with the angles calculated from Ungemach's elements, are given in Table 11.

TABLE 10. CORNETITE: $\text{Cu}_3\text{PO}_4(\text{OH})_3$ Orthorhombic, *Pbca* $a:b:c=0.7715:1:0.5048$; $p_0:q_0:r_0=0.6544:0.5048:1$

Form	ϕ	$\rho=C$	ϕ_1	$\rho_1=A$	ϕ_2	$\rho_2=B$
<i>c</i> (001)	—	0° 00'	0° 00'	90° 00'	90° 00'	90° 00'
<i>b</i> (010)	0° 00'	90 00	90 00	90 00	—	0 00
<i>a</i> (100)	90 00	90 00	—	0 00	0 00	90 00
<i>m</i> (110)	52 21	90 00	90 00	37 39	0 00	52 21
<i>d</i> (210)	68 54½	90 00	90 00	21 05½	0 00	68 54½
<i>n</i> (021)	0 00	45 16½	45 16½	90 00	90 00	44 43½
<i>e</i> (102)	90 00	18 07	0 00	71 53	71 53	90 00
<i>v</i> (121)	32 57	50 16	45 16½	65 16½	56 48	49 48½
<i>p</i> (221)	52 21	58 49½	45 16½	47 21½	37 23	58 29½
<i>r</i> (321)	62 47	65 38	45 16½	35 54	26 59½	65 22½
<i>s</i> (421)	68 54½	70 23	45 16½	28 30	20 54½	70 11
<i>t</i> (521)	72 51	73 43	45 16½	23 28½	16 59½	73 33½

Ungemach's observed forms listed approximately in order of decreasing importance are:

Ungemach (110), (111), (104), (102), (112), (001), (021), (100), (010), (113), (114)
 Structure (021), (121), (210), (110), (221), (100), (102), (010), (001), (321), (421)

The first three are also the most important observed by Cesàro, Hutchinson & MacGregor and Schoep. Donnay¹ states that the morphological analysis confirms Ungemach's unit and predicts the space group *Pbcn* with one anomaly; namely, (104) more important than (102). This is an

TABLE 11. CORNETITE, KATANGA

Comparison of Measured and Calculated angles

	Measured	Calculated
<i>n</i> (021): <i>n</i> (021)	90° 43'	90° 33'
<i>n</i> (021): <i>v</i> (121)	24 53	24 43½
<i>n</i> (021): <i>p</i> (221)	41 36	42 38½
<i>n</i> (021): <i>t</i> (521)	67 20	66 31½
<i>v</i> (121): <i>t</i> (521)	41 55	41 48
<i>p</i> (221): <i>t</i> (521)	26 10	23 53

¹ Personal communication April 8, 1948.

established fact as (104) (Ungemach) was observed by earlier authors and is more important on the crystals used in this study, while (102) has been observed only by Ungemach as a less important form. Transformed to the structural setting this space group becomes $Pbca$ as determined by x -ray methods and (104) becomes (210) which is more important than (110) as expected in this space group. However, the important form (111) Ungemach becomes (121) and is anomalous in the structural setting.

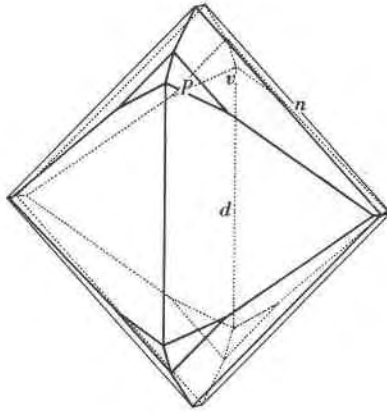


FIG. 8. Cornetite, Bwana Mkubwa, Northern Rhodesia; crystal showing the forms $s(210)$, $n(021)$, $v(121)$ and $p(221)$.

Composition and Cell Content. The structural lattice dimensions together with the measured specific gravity of cornetite, 4.10 (Hutchinson & MacGregor, 1913, 1921) give the molecular weight of the cell contents, $M = 2693.6$. In Table 12 this value has been used to obtain the atomic contents of the unit cell from the one published analysis of cornetite.

TABLE 12. CORNETITE: ANALYSIS AND CELL CONTENT

$M = 2693.6$

	1	2		3	4
CuO	71.30	24.15	Cu	24.15	24
P ₂ O ₅	19.96	3.79	P	7.58	8
H ₂ O	8.73	13.04	H	26.08	24
	<u>99.99</u>		O	56.14	56

1. Bwana Mkubwa, Northern Rhodesia; anal. Hutchinson & MacGregor (1921).
2. Unit cell content. 3. Atoms in the unit cell. 4. Ideal cell content for $8[\text{Cu}_3\text{PO}_4(\text{OH})_3]$.

TABLE 13. CORNETITE— $\text{Cu}_3\text{PO}_4(\text{OH})_3$: X-RAY POWDER PATTERN
 Orthorhombic, $Pbca$; $a=10.88$, $b=14.10$, $c=7.11$ Å; $Z=8$

I	$\theta(\text{Cu})$	$d(\text{meas.})$	(hkl)	$d(\text{calc.})$	I	$\theta(\text{Cu})$	$d(\text{meas.})$	(hkl)	$d(\text{calc.})$
5	8.07°	5.48 Å	(111)	5.483 Å	3	16.30°	2.74 Å	(131)	2.744 Å
			(200)	5.440				(222)	2.742
6	8.74	5.07	(210)	5.075				(241)	2.731
			(021)	5.006	3	17.65	2.54	(302)	2.539
3	9.74	4.55	(121)	4.548				(420)	2.538
9	10.34	4.29	(220)	4.307				(250)	2.504
7	12.09	3.68	(131)	3.689	2	17.95	2.50	(042)	2.503
			(221)	3.684				(411)	2.500
			(230)	3.556				(312)	2.499
1	12.64	3.53	(002)	3.555	3	18.45	2.44	(142)	2.439
			(040)	3.525				(431)	2.235
			(231)	3.181	2	20.22	2.23	(332)	2.234
			(022)	3.174				(061)	2.231
8	14.09	3.17	(041)	3.158				(402)	2.160
			(311)	3.149	3	21.0	2.15	(260)	2.157
			(122)	3.047				(440)	2.153
10	14.69	3.04	(141)	3.033				(213)	2.147
			(240)	2.958				(261)	2.064
5	15.15	2.95	(321)	2.937	7	22.0	2.06	(342)	2.060
								(441)	2.061
								(511)	2.058

I	$\theta(\text{Cu})$	$d(\text{meas.})$	I	$\theta(\text{Cu})$	$d(\text{meas.})$	I	$\theta(\text{Cu})$	$d(\text{meas.})$
2	23.15°	1.959 Å	1	32.21°	1.445 Å	1	50.33°	1.001 Å
1	23.96	1.897	2	32.92	1.418	$\frac{1}{2}$	52.15	0.975
$\frac{1}{2}$	24.86	1.833	1	34.23	1.369	$\frac{1}{2}$	52.75	0.968
2	25.47	1.791	1	35.43	1.329	2	53.66	0.956
2	26.27	1.740	1	37.45	1.266	$\frac{1}{2}$	55.77	0.932
1	26.88	1.703	1	38.25	1.244	2	63.72	0.859
4	29.29	1.574	2	39.16	1.219	2	69.86	0.821
4	29.90	1.545	$\frac{1}{2}$	40.17	1.193	$\frac{1}{2}$	76.20	0.794
3	30.70	1.509	1	47.01	1.053	1	83.75	0.775
1	31.51	1.471	1	48.12	1.034			

The total number of oxygen atoms is clearly 56, thus the true cell content may be represented by the structural formula



Column 2 indicates the cell content of H_2O to be 13, however this would require a total oxygen content of 57 which is incompatible with the symmetry of the space group $D_{2h}^{15}-Pbca$. The cell content given in

column 4 above gives the calculated specific gravity, 4.100, in agreement with the measured value. This affords complete confirmation of the structural formula given here and the simpler empirical formula suggested by Hutchinson & MacGregor (1921) rather than the more complex formula, $2\text{Cu}_3(\text{PO}_4)_2 \cdot 7\text{Cu}(\text{OH})_2$.

X-ray Powder Pattern. Table 13 gives the observed relative intensities and measured spacings of the observed diffractions for the *x*-ray powder spectrum of cornetite (Fig. 7). The pattern has been indexed as far as $\theta = 22.0^\circ$; the measured spacings agree satisfactorily with one or more spacings calculated from the lattice dimensions and thus the pattern is adequately verified.

Optical Properties. The optical data on cornetite given by Cesàro (1912) and Hutchinson & MacGregor (1921) have been supplemented by new observations by Larsen & Berman (1934). A re-statement of the optical properties with reference to the new structural setting of cornetite may properly be given here. Observations on a typical crystal from Northern Rhodesia, mounted on a universal stage, confirmed this orientation of the ellipsoid in the structural setting.

$X = b[010]$	$\alpha = 1.765$ (green)	negative
$Y = a[100]$	$\beta = 1.81$	$2V = 33^\circ$ (TI)
$Z = c[001]$	$\gamma = 1.82$	$r < v$ strong

REFERENCES

- ARFVEDSON (1825): *Mineralogie—Berzelius' Jahresber.*, **4**, 140–175.
- BARTH, T. & BERMAN, H. (1930): Neue optische Daten wenig bekannter Minerale. (Die Einbettungsmethode).—*Chemie der Erde*, **5**, 22–42.
- BERGEMANN, C. (1828): Chemische Untersuchungen und mineralogische Bemerkungen über verschiedene phosphorsaure Kupfer—*Schweigg. Jour.*, **54**, 305–324.
- (1858): Bemerkungen über phosphorsaures Kupferoxyd—*Ann. Phys. Chem.*, **104**, 190–192.
- (1858): Über den Ehlit—*N. Jb. Min.*, 191–195.
- BUTTGEBACH, H. (1916): *Les minéraux et les roches*—Liège.
- CESÀRO, G. (1912a): Sur un nouveau minéral du Katanga—*Ann. Soc. géol. Belgique*, **39**, pp. B241–B242.
- (1912b): Sur un nouveau minéral du Katanga—*Ann. Soc. géol. Belgique*, annexe to **39**, pp. 41–48 (Publ. rel. Congo Belge).
- & BELLIERE, M. (1922): Sur le diaspore, la libéthénite et quelques autres minéraux du Katanga—*Ann. Soc. géol. Belgique*, **45**, 172–182 [*M.A.*, **2**, 226].
- CHURCH, A. H. (1864): Revision of the mineral phosphates—*Chem. News*, **10**, 217.
- (1873): New analyses of certain mineral arseniates and phosphates—*Jour. Chem. Soc.*, **26**, 101–111.
- DANA, J. D. (1882): *System of Mineralogy*—ed. 5—New York.
- DANA, J. D. & E. S. (1892): *System of Mineralogy*—ed. 6—New York.
- FIELD, F. (1859): On the occurrence of tagilite and libethenite, as well as some combinations of lime, copper, and phosphoric acid, in a mine near Coquimbo, Chile—*Chem. Gaz.*, **17**, 225.

- HAUSMANN, J. F. L. (1813): *Handbuch der Mineralogie*, 3 vols.—Gottingen.
- HEDDLE (1855): Analysis of lunnite from Cornwall—*Phil. Mag.*, **10**, 39.
- HERMANN, R. (1846): Untersuchungen russischer Mineralien—*J. Prakt. Chem.*, **37**, 175–193.
- HUTCHINSON, A. & MACGREGOR, A. M. (1913): A crystalline basic copper phosphate from Rhodesia—*Nature*, **92**, 364.
- (1921): On cornetite from Bwana Mkubwa, Northern Rhodesia—*Min. Mag.*, **19**, 225–232.
- KÜHN, O. B. (1840): Phosphorsaures Kupferoxyd—*Ann. Chem. Pharm.*, **34**, 218–220.
- (1844): Ueber einige natürliche phosphorsaure und arsensaure Kupfersalze—*Ann. Chem. Pharm.*, **51**, 123–132.
- LACROIX, A. (1910): *Minéralogie de la France et de ses colonies*, vol. 4—Paris.
- LARSEN, E. S. (1921): The microscopic determination of the nonopaque minerals—*U. S. Geol. Surv.*, Bull. **679**.
- LARSEN, E. S. & BERMAN, H. (1934): The microscopic determination of the nonopaque minerals—*U. S. Geol. Surv.*, Bull. **848**.
- MASKELYNE, S. & FLIGHT (1872): Mineralogical notices—*Jour. Chem. Soc.*, **25**, 1057.
- NORDENSKIÖLD, A. E. (1858): Undersökning af några vid Nischni-Tagil förekommande kopparfosfater—*Acta Soc. Scient. Fenn.*, **5**, 335–341.
- RAMMELSBURG, C. (1860): *Handbuch der Mineralchemie*, ed. 1—Leipzig.
- (1875): *Handbuch der Mineralchemie*, ed. 2—Leipzig.
- RHODIUS, R. (1847): Untersuchung des Phosphorochalcits, Ehlits und eines natürlichen Bleioxyd-Chlorbleis—*Ann. Chem. Pharm.*, **62**, 369–374.
- SCHOEP, A. (1922): On the absence of cobalt in cornetite from Katanga, Belgian Congo—*Min. Mag.*, **19**, 301–302.
- (1927): Kristallen van Cornetiet en hunne brekingsindices—*Natuurwetenschappelijk Tijdschrift, Antwerpen*, **9**, 125–128.
- SCHRAUF, A. (1879): Ueber Phosphorkupfererze—*Zeits. Kryst.*, **4**, 1–33.
- UNGEMACH, H. (1929): Précisions cristallographiques sur quelques minéraux du Congo Belge—*Ann. Soc. géol. Belgique (Publ. rel. Congo Belge)*, **52**, c75–c85.